THE JOURNAL OF PHYSICAL CHEMISTRY B

ARTICLE

pubs.acs.org/JPCB

Update of the Cholesterol Force Field Parameters in CHARMM

Joseph B. Lim, Brent Rogaski, and Jeffery B. Klauda*

Department of Chemical and Biomolecular Engineering, University of Maryland, College Park, Maryland 20742, United States

Supporting Information

ABSTRACT: A modification of the CHARMM36 lipid force field (C36) for cholesterol, henceforth, called C36c, is reported. A fused ring compound, decalin, was used to model the steroid section of cholesterol. For decalin, C36 inaccurately predicts the heat of vaporization (~10 kJ/mol) and molar volume (~10 cc/mol), but C36c resulted in near perfect comparison with experiment. MD simulations of decalin and heptane at various compositions were run to estimate the enthalpy and volumes of mixing to compare to experiment for this simple model of cholesterol in a chain environment. Superior estimates for these thermodynamic properties were obtained with C36c versus C36. These new parameters were applied to cholesterol, and quantum mechanical calculations were performed to modify the torsional potential of an acyl chain torsion for cholesterol. This model was tested through simulations of DMPC/10% cholesterol, DMPC/30% cholesterol, and DOPC/10% cholesterol. The C36 and C36c results were similar for surface areas per lipid, deuterium order parameters, electron density profiles, and atomic form factors and generally agree well with experiment. However, C36 and C36c produced slightly different cholesterol angle distributions with C36c adopting a more perpendicular orientation with respect to the bilayer plane. The new parameters in the C36c modification should enable more accurate simulations of lipid bilayers with cholesterol, especially for those interested in the free energy of lipid flip/flop or transfer of phospholipids and/or cholesterol.

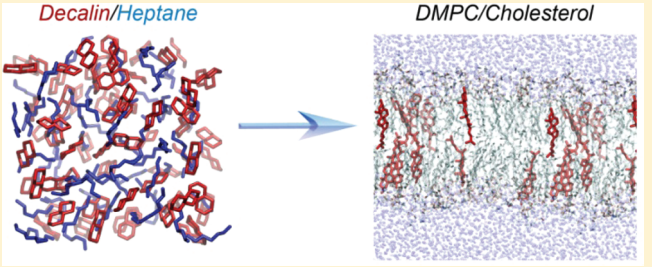

1. INTRODUCTION

Cholesterol is a specific sterol that has a steroidal ring structure with a polar headgroup (hydroxyl) and a branched acyl chain (Figure 1). The amphiphilic nature of cholesterol combined with other lipids, such as phospholipids, can result in lamellar structures at fully hydrated conditions. Cholesterol is the primary sterol in humans, and other organisms contain similar sterols, such as ergosterol in yeast.[1] Although dietary sources of cholesterol are of concern for health, the primary source of cholesterol in the body is through synthesis and distribution via lipoproteins. For some single-celled organisms, the endoplasmic reticulum is the primary source of sterols.[2]

The primary functional use of cholesterol and other sterols is in cellular membranes. The concentrations of cholesterol can vary depending on the organism. For example, some organisms lack the ability to make sterols and thus lack these in their membranes, while others such as Chlamydia have elevated levels in the outer membranes.[3] Many internal cellular organelles contain low levels of sterols (endoplasmic reticulum and mitochondrion), but levels in the plasma membrane are typically the highest (30% or greater).[1] Cholesterol is even a majority lipid in ocular lens membranes.[4,5] Aside from increasing membrane rigidity and chain order,[6] cholesterol at certain concentrations can lead to phase separation into cholesterol-poor (liquid disordered) and -rich (liquid ordered) domains or rafts.[2,7] Certain transmembrane proteins or protein anchors have preference for liquid ordered/disordered domains, and these lipid structures can be important in cell signaling.[2]

Molecular simulations of cholesterol-containing membranes have been used to study cholesterol's influence on various membrane properties,[8,9] formation of rafts or nanodomains,[10−13] and mechanisms and energetics of cholesterol flip/flop.[14,15] Molecular dynamics (MD) simulations utilize force fields to describe molecular interactions and thus motions. The CHARMM force field considers all atoms (including hydrogen) and has been well-developed for typical phospholipids.[16] The cholesterol force field in CHARMM that was developed by Pitman et al.[17] essentially used CHARMM27 parameters for alkanes and alkenes and protein force field parameters for threonine for the hydroxyl and applied these to cholesterol. Bond and angle potentials were fit to crystal structures of the steroidal section of cholesterol and torsional angles for the hydroxyl group were modified based on quantum mechanical calculations. Although this parameter set for cholesterol was successfully used in 1-stearoyl-2-docosahexaenoyl-*sn*-glycero-3-phosphocholine bilayers with cholesterol,[17] the main limitation with this force field was the transference of inaccurate Lennard-Jones (LJ) parameters for the fused rings of cholesterol (see below). Recent updates to the CHARMM force field for ligands (CHARMM General Force Field, CGenFF)[18] required some adjustment of LJ parameters to obtain accurate heats of vaporization and molar volumes of cyclic molecules.

Received: August 17, 2011
Revised: November 4, 2011
Published: December 03, 2011

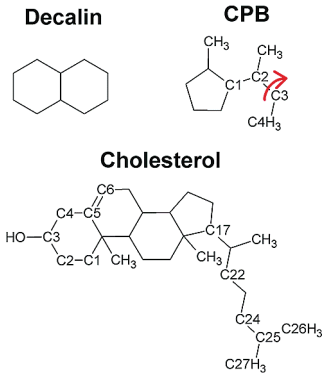

Figure 1. Model compounds to develop and test modifications to the cholesterol force field. CPB = cyclo-propane branched model.

Table 1. Amounts of Decalin and Heptane for the Decalin/Heptane Simulations

mole fraction of decalin	0.90	0.80	0.70	0.60	0.50	0.40	0.30	0.20	0.10
decalin	115	102	90	77	64	51	38	26	13
heptane	13	26	38	51	64	77	90	102	115

As described in this article, adjustment of the LJ terms for cholesterol is needed based on small molecule tests.

Small molecule simulations of a fused ring molecule (decalin in Figure 1) are used initially to develop a more accurate cholesterol force field in CHARMM. The methods used in these simulations and those with lipid bilayers are described in section 2. The results are subdivided into simulations to describe the development of the cholesterol force field and then bilayer simulations to verify the validity of this new set of parameters. The results are discussed and conclude with comments regarding previous CHARMM27-based simulations with cholesterol.

2. METHODS

Quantum mechanical (QM) calculations of small molecule conformational energies were calculated using the Gaussian03 suite of programs.[19] Details regarding the QM methods for these energies are given in section 3.1.3.

MD simulations of decalin, heptane, and their mixtures were performed. For the decalin- and heptane-only simulations, 160 and 64 molecules, respectively, were placed in a 45 × 45 × 45 Å cubic unit cell and minimized in CHARMM[20] using the Steepest Descent (SD) algorithm for 200 steps. An equilibration trajectory was then generated using CHARMM and the CHARMM36 (C36) lipid force field[16] in the NPT (constant number of molecules, pressure, and temperature) ensemble. Heptane was simulated at 1 bar and 298.15 K for 5 ns, and decalin was simulated at 1 bar and at 295.15 and 298.15 K for 5 and 6 ns, respectively. The compositions of all decalin/heptane mixtures, each of which was placed in a 45 × 45 × 45 Å cubic unit cell, are shown in Table 1. All mixtures were minimized in CHARMM using the SD algorithm for 2000 steps and the Adopted Basis Newton−Raphson (ABNR) algorithm for 2000 steps. An equilibration trajectory at 298.15 K was generated using CHARMM for each mixture for 210 ps. Three independent runs, starting from the last frame of the equilibration and each with a different initial velocity seeding, were performed for each mixture. The production run length for each simulation and composition was 21−25 ns. For these triplicate simulations of decalin/heptane mixtures, C36 and a modification of the C36 lipid force field parameters, henceforth, named CHARMM36c (C36c), were used.

Table 2. Lipid, Water Amounts, and Production Lengths of Bilayer Simulations

bilayer	DMPC/ 10% cholesterol	DMPC/ 30% cholesterol	DOPC/ 10% cholesterol
DMPC	90	70	0
DOPC	0	0	90
cholesterol	10	30	10
water (C36c/C36)	2998/2998	3011/2998	2996/2996
production run length (ns, C36c/C36)	40/40	100/50	45/45

The CHARMM-GUI Membrane Builder[21,22] was used to generate membrane coordinates for mixtures of dimyristoylphosphatidylcholine (DMPC) and dioleoylphosphatidylcholine (DOPC) with cholesterol (see Table 2). A hydration of 30 TIP3P model waters per lipid was used. For each bilayer system, coordinates were first minimized in CHARMM using the SD algorithm for 1000 steps followed by the ABNR algorithm for 2000 steps. An equilibration trajectory at 298.15 K was generated for 1 ns using NAMD.[23] A production run was then performed until 25 ns of equilibrated trajectory data were obtained as indicated by the area per lipid (all with NAMD). The C36 lipid force field was used for all bilayer simulations, both with and without the C36c modification. A tetragonal unit cell was used to maintain an equal dimension between X and Y (in the plane of the membrane), while Z varied independently.

The van der Waals (vdW) interactions were smoothly switched off at 10−12 Å by a forced-based switching function. Long-range electrostatic interactions were calculated using the particle-mesh Ewald (PME) method.[24] All simulations of decalin, heptane, or mixtures thereof were generated using a time step of 1 fs, while all bilayer simulations were generated using a time step of 2 fs. Simulations of decalin, heptane, and related mixtures used the Hoover thermostat[25] to maintain constant temperature and the Nosé−Hoover piston[26,27] to maintain constant pressure at 1 bar. Since long-range vdW interactions are important for alkanes[28] and long-range vdW are typically used in model development in CHARMM,[29,30] the isotropic periodic sum method[28,31] was used for all small molecule simulations. Force-based cutoffs were used for the bilayers to be consistent with the C36 lipid force field.[16] For the bilayer simulations, Langevin dynamics was used to maintain constant temperatures for each system, while the Nosé−Hoover Langevin-piston algorithm[32,33] was used to maintain constant pressure at 1 bar. An interpolation order of 4 and a direct space tolerance of 10^{-6} were also used for the PME method for the bilayer simulations.

After completion of all simulations, the simulations of decalin, heptane, and mixtures thereof were analyzed for molar volume, heat of vaporization, and heat of mixing. For decalin, simulations of each individual molecule in a given coordinate set were used to obtain the energy of each molecule in the ideal gas phase. This was necessary to obtain the heat of vaporization, given by

$$\Delta H_{vap} = \langle E_{ind} \rangle - \langle E \rangle + RT \quad (1)$$

Table 3. Density and Heat of Vaporization of Decalin from Simulation and Experiment

	C36 lipid[16]		CGen FF[18]		expt[34]	
	295.15 K	298.15 K	295.15 K	298.15 K	295.15 K	298.15 K
density (cc/mol)	163.961	164.546	157.302	157.612	154.211	159.660
heat of vaporization (kcal/mol)	7.50		9.98		9.88	

where $\langle E_{ind} \rangle$ is the average energy of all the individual molecule simulations, $\langle E \rangle$ is the average energy of the 160-molecule simulation (normalized by the number of molecules in the simulation), R is the gas constant, and T is temperature. The excess molar enthalpy is given by

$$H^{ex} = U^{ex} - PV^{ex} \quad (2)$$

where U^{ex} is the excess molar internal energy, P is pressure, and V^{ex} is the excess molar volume. The excess molar internal energy and excess molar volume are given by

$$U^{ex} = U_{mix} - x_{c7}U_{c7} - x_dU_d \quad (3)$$

$$V^{ex} = V_{mix} - x_{c7}V_{c7} - x_dV_d \quad (4)$$

where U_{mix}, U_{c7}, and U_d are the molar internal energy of the mixture, pure heptane, and pure decalin, respectively, and similarly, the molar volumes are V_{mix}, V_{c7}, and V_d. x_{c7} is the mole fraction of heptane in the mixture, and x_d is the mole fraction of decalin in the mixture.

The bilayer simulations were analyzed for the overall surface area (SA) per lipid, deuterium order parameters, atomic form factors, electron density profiles, and cholesterol angle distributions. The deuterium order parameters are calculated via the following equation:

$$|S_{CD}| = \left(\frac{1}{2}\right)\langle 3\cos^2\theta - 1\rangle \quad (5)$$

where θ is the angle of a C−H vector with respect to the bilayer normal. Deuterium order parameters are typically reported as absolute value, and this is assumed in our abbreviation (S_{CD}). The cholesterol angle in this study was defined as the angle between the vector formed by the C3 and C17 atoms and the z axis.

3. RESULTS

3.1. Cholesterol Force Field Development. *3.1.1. Decalin Force Field.* As a representation of the steroidal ring in cholesterol, decalin (Figure 1) was simulated using parameters from the C36 lipid force field (referred to here as C36) as well as the CHARMM General Force Field (CGenFF)[18] without modifications. The results, as well as relevant experimental results,[34] are shown in Table 3. The densities calculated from the C36 differed from the experimental measurements at 295.15 and 298.15 K by approximately 10 cc/mol and 5 cc/mol, respectively. The C36 heat of vaporization also deviated significantly from experiment, with a difference of approximately 2.4 kcal/mol at 295.15 K.

By contrast, the densities calculated from the CGenFF differed from experiment[34] by approximately 3 cc/mol and 2 cc/mol at 295.15 and 298.15 K, respectively. Moreover, the heat of vaporization calculated from the CGenFF simulation virtually matched the experimental measurement at 295.15 K. On the basis of these results, it was determined that parameters from

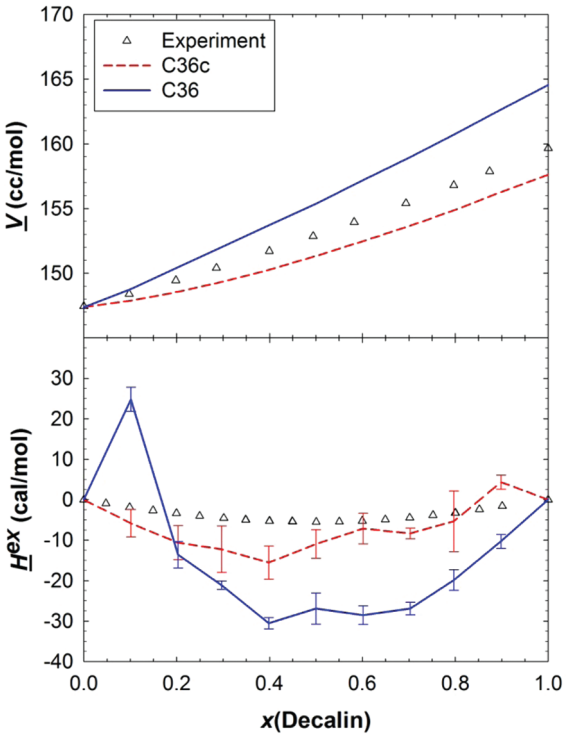

Figure 2. Top: molar volume of decalin/heptane mixtures. Bottom: excess molar enthalpy of decalin/heptane mixtures. MD simulations are compared to experiment in symbols.[35,36]

CGenFF for decalin were required to obtain accurate fluid phase properties. Thus, these parameters were used in the decalin/heptane simulations. Details of the parameters for decalin can be found in the Supporting Information.

3.1.2. Decalin/Heptane Model for the Interior Bilayer. Since the C36 lipid chains are based on pre-CGenFF parameters for alkanes, standard mixing rules for atoms between alkane and decalin may not be sufficient to describe their interaction. Initially, CGenFF-based decalin was simulated with C36-based alkanes, but agreement with experiment of mixture volumes and excess enthalpy was unsatisfactory. From experiment[35,36] at an equal molar composition, the volume and H^{ex} are 152.9 cc/mol and −5.5 cal/mol, but with CGenFF/C36, these were calculated to be 150.8 cc/mol and −193 cal/mol. To avoid the need to reparameterize the lipid acyl chains to be consistent with that in the CGenFF, simulations of decalin/heptane mixtures were undertaken to optimize the relevant nonbonded mixing parameters with the NBFIX command in CHARMM. This was done by determining the optimal weighted average of parameters between CGenFF (decalin) and C36 (heptane). Simulations with various weighted averages of the mixing parameters were performed, and a weighted average of 10% C36/90% CGenFF for the ε/k was found to best match experiment. The relevant

dx.doi.org/10.1021/jp207925m | J. Phys. Chem. B 2012, 116, 203–210

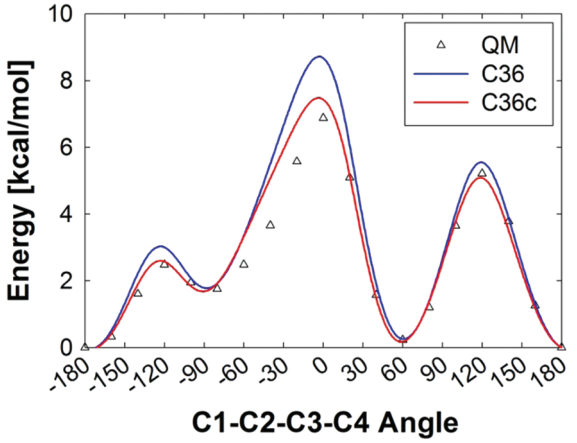

Figure 3. Conformational energies of the C1−C2−C3−C4 torsion of CPB calculated from QM (CCSD(T)/cc-pVQZ), C36, and fit to QM data (C36c).

parameters are shown in the Supporting Information and are referred to here as C36c. The molar volume and excess enthalpy of decalin/heptane mixtures are shown in Figure 2. Results using the C36c are compared to results using C36 for decalin and heptane, as well as experimental data.[35,36] Since there is some error regarding the molar volume of decalin with C36c, the pure data point is slightly off compared to experiment. However, this is an improvement from C36, especially for compositions similar to the lipid environment (less than 50%). (Note that for pure decalin, the difference between C36 and C36c is only the new LJ terms in the Supporting Information, Table S4.) The excess enthalpy is much improved with the C36c (Figure 2). The H^{ex} was overestimated and of the wrong sign for C36 and agrees better with experiment for C36c. The large error at low concentrations of decalin will likely create inaccuracies for C36 bilayer simulations with cholesterol, especially enthalpies of the mixture in a similar concentration range.

3.1.3. QM Calculations. With decalin as a model of the steroidal moiety of cholesterol, the chain attached to these fused rings was investigated to determine if the torsional potential in CHARMM is appropriate. A branched acyl-chain attached to cyclopropane was used to model torsions for cholesterol's chain (CPB in Figure 1). The torsional energy was calculated using high-level QM based on a previously developed hybrid method that results in effective CCSD(T)/cc-pVQZ energies.[37] The C1−C2−C3−C4 torsion was the only torsion modified from C36-based parameters (others were deemed accurate with existing parameters). Figure 3 compares the QM energies with C36 and C36c (fit to QM data). Although overall C36 agrees with the QM energies, the torsional barriers between trans and gauche are overestimated. The width of the well for gauche is also smaller with C36. These changes will influence the transition time between trans and gauche, and MD simulations with cholesterol should better sample these minima.

3.2. MD Simulations of Lipid Bilayers. *3.2.1. Surface Area Per Lipid.* Decalin provides a good model compound for cholesterol's ring structure, and heptane provides a good model for the acyl-chains of the phosphoplid. Therefore, these small molecule studies enable evaluation of the effectiveness of the new parameters with simulations of DMPC/10% cholesterol, DMPC/30% cholesterol, and DOPC/10% cholesterol. MD simulations of these three bilayers were performed using C36 for the lipid and

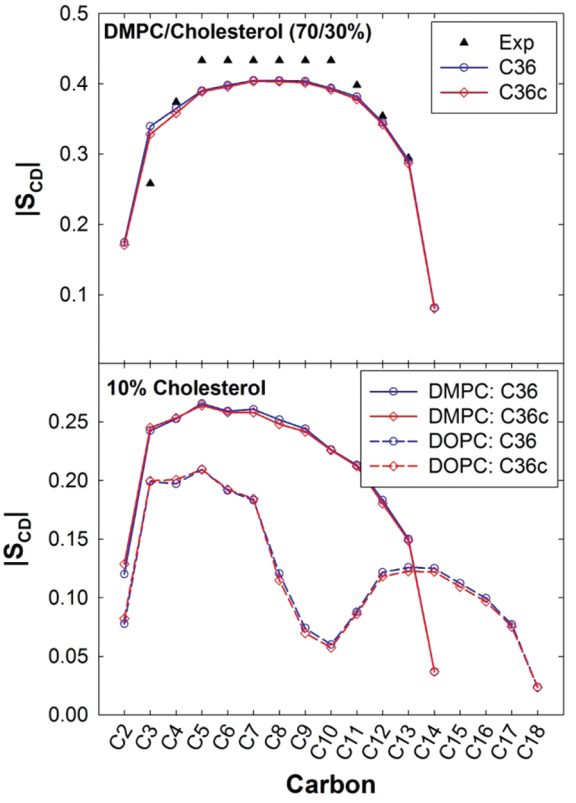

Figure 4. Average deuterium order parameters of the *sn*-2 chain of the phospholipid (splitting at C2 carbon is shown). Top: DMPC with 30% cholesterol for MD simulations and experiment.[41] Bottom: DMPC and DOPC with 10% cholesterol. Standard error bars did not exceed the size of the data symbols and are not shown.

cholesterol, as well as duplicate simulations using C36c for cholesterol (details of applying C36c to cholesterol can be found in the Supporting Information). The average SA per lipid (total area divided by number of lipids including cholesterol per leaflet) was used not only to calculate a key bilayer property but also to determine whether the bilayer trajectories were sufficiently equilibrated for analysis. For C36, DMPC/10% cholesterol, DMPC/30% cholesterol, and DOPC/10% cholesterol had average SAs per lipid of 55.8 ± 0.2, 42.6 ± 0.1, and 64.2 ± 0.2 Å^2/lipid, respectively. For the C36c modification, these same bilayers had average SAs per lipid of 56.1 ± 0.1, 43.0 ± 0.1, and 64.9 ± 0.2 Å^2/lipid, respectively. The last 20 ns of each of the C36 simulations and the last 25 ns of each of the C36c simulations were found to be relatively stable and proof of a sufficiently equilibrated trajectory (data not shown). The SAs for DMPC and cholesterol were statistically identical for C36 and C36c and slightly larger for C36c for cholesterol with DOPC.

3.2.2. Phospholipid Deuterium Order Parameters. Deuterium order parameters (S_{CD}) were calculated to provide a quantitative measure of chain order for the aliphatic chains of the phospholipids. S_{CD} parameters are shown for the *sn*-2 chain of each of the bilayer systems studied in Figure 4. There were minimal differences between C36 and C36c. Both force fields slightly underestimate the order parameters compared to experiment.[38] The deuterium order parameters of the aliphatic chains followed expected trends. DMPC/30% cholesterol had the highest overall order and closely matched experimental data. DMPC/10% cholesterol had significantly lower order, though the shape of

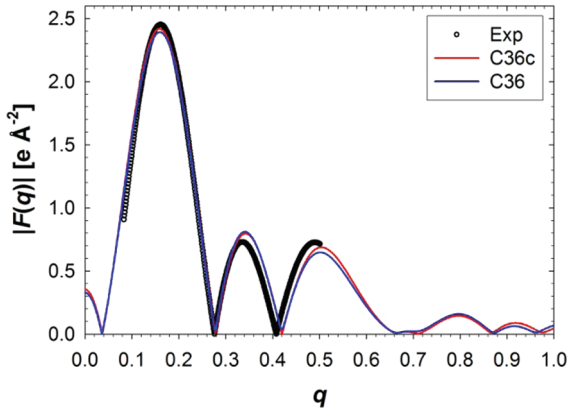

Figure 5. Form factors for DMPC/10% cholesterol bilayers compared to experiment.[39]

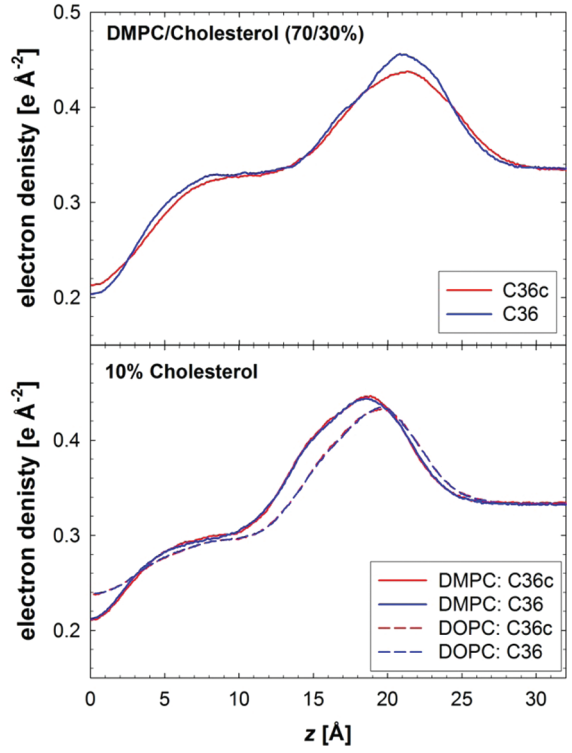

Figure 6. Electron density profiles of DMPC/10% cholesterol, DMPC/30% cholesterol, and DOPC/10% cholesterol.

the profile is similar to that of DMPC/30% cholesterol. DOPC/10% cholesterol, as expected, had the lowest overall order, due to the single double bond at the carbon 9 and 10 positions in each of its chains. A precipitous drop in chain order is observed at these positions.

3.2.3. Form Factors and Electron Density Profiles. Form factors were calculated for DMPC/10% cholesterol to allow comparison to small-angle X-ray scattering data from experiment[39] (Figure 5). There appears to be very good agreement between the calculated $F(q)$ (C36 and C36c) and from experiment. The identical SAs per lipid for C36 and C36c for DMPC/10% cholesterol also appear to suggest there is minimal change in the overall structure of the bilayer between these two force fields.

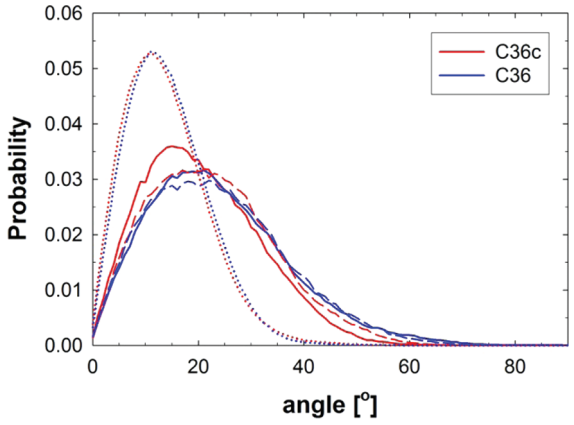

Figure 7. Cholesterol angle distributions of DMPC/10% cholesterol (solid), DMPC/30% cholesterol (dotted), and DOPC/10% cholesterol (dashed).

While atomic form factors offer a direct comparison of simulation to experiment of bilayer structure, electron density profiles provide more direct information, such as average membrane thickness and the location of particular lipid components. Electron density profiles were calculated for each of the bilayer systems studied (Figure 6), as well as individual lipid component densities (Supporting Information, Figures S1, S2, and S3). As suggested by the atomic form factors, the DMPC/10% cholesterol density is essentially identical for C36 and C36c. The only simulation that has a minor change in density is DMPC/30% cholesterol. For this simulation, the methyl trough at the center of the bilayer was increased for C36c, suggesting more leaflet overlap. The component densities (cholesterol, phosphate, and choline) are more broad (Supporting Information, Figure S3) with C36c and thus result in a less sharp peak for the maximum in density (Figure 6). The phospholipid headgroup region ($|Z| \approx$ 22 Å) illustrates the effects of cholesterol concentration. The shoulder of the peak in this region lies more toward the center of the membrane in DMPC/10% cholesterol, whereas this same feature shifts to the outside of the membrane in the C36c simulation of DMPC/30% cholesterol.

At the low-density trough (Z = 0 Å), for both C36 and C36c, DOPC/10% cholesterol had the greatest density, followed by DMPC/30% cholesterol and then DMPC/10% cholesterol. For C36c, DMPC/30% cholesterol had the greatest peak-to-peak distance (42.6 Å), followed by DOPC/10% cholesterol (39.1 Å) and then DMPC/10% cholesterol (37.7 Å). For C36, the trend was the same (43.1, 39.05, and 37.05 Å, respectively). Both C36c and C36 agree favorably with experiment at 303 K (41.8 ± 0.4, 37.0 ± 0.5, and 38.2 ± 0.5 Å, respectively).[6]

3.2.4. Cholesterol Structure in Bilayers. Cholesterol angle distributions were also calculated for each of the bilayer simulations to compare the effect of our force field modification to C36. A cholesterol angle of 90° indicates a cholesterol molecule completely parallel to the bilayer surface, while an angle of 0° indicates a cholesterol molecule completely perpendicular to the surface. The cholesterol angle distributions are shown in Figure 7.

DOPC/10% cholesterol, with a double bond in each of its acyl chains, is expected to show cholesterol favoring a less perpendicular position than in other bilayers because of its increased chain disorder disfavoring upright cholesterol. Indeed, the distributions in Figure 7 show this to be the case. For the C36c simulations,

Table 4. Cholesterol Deuterium Order Parameters[a]

carbon position	DMPC/10% cholesterol		DMPC/30% cholesterol		DMPC/30% cholesterol (C36)		DMPC/30% cholesterol (exptl)[40]		DOPC/10% cholesterol	
C2	0.229	0.327	0.250	0.386	0.245	0.365	0.268	0.378	0.228	0.315
C3	0.3575		0.417		0.397		0.404		0.345	
C4	0.150	0.32	0.181	0.364	0.194	0.354	0.249	0.378	0.13	0.30
C6	0.03		0.035		0.059		0.026		0.02	
C22	0.21		0.359		0.360		0.416		0.22	
C24	0.28	0.112	0.252	0.332	0.236	0.331	0.252	0.322	0.11	0.251
C26	0.005		0.024		0.024		0.021		0.005	
C27	0.004		0.010		0.016		0.024		0.007	

[a] All data is for C36c unless otherwise noted. Error bars are 0.01 or less and not reported. The presence of two values for one carbon position indicates the two different values calculated for the two carbon−hydrogen bonds. A single value is either an average or indicative of one carbon−hydrogen bond.

DOPC/10% cholesterol had the highest mode angle (21°), followed by DMPC/10% cholesterol (15°), and then DMPC/30% cholesterol (11°). For C36, the trend was the same, though the values of the modes were slightly different, with mode angles of 22°, 21°, and 11° for DOPC/10% cholesterol, DMPC/10% cholesterol, and DMPC/30% cholesterol, respectively. As expected, higher cholesterol concentrations lead to the upright, perpendicular position to be favored for cholesterol, which consequently results in more lipid chain order.

The deuterium order parameters for particular carbon positions in cholesterol (Figure 1) are shown in Table 4. As with the aliphatic chains, the cholesterol order parameters seem to reflect expected trends, with DOPC/30% cholesterol having the highest overall S_{CD}, followed by DMPC/10% cholesterol, and then DOPC/10% cholesterol (both C36c and C36). The order parameters for DMPC/30% cholesterol (both C36c and C36) are in quantitative agreement with the experimental data,[40] lending credence to the order parameters calculated from the simulations. The splitting of the S_{CD}s at carbon positions 2, 4, and 24 are well reproduced with both force fields.

4. DISCUSSION AND CONCLUSIONS

In general, the C36c modification improves the accuracy of the current lipid force field for CHARMM, as illustrated by the simulations of decalin and heptane. While the C36 overestimates the experimental molar volume of a decalin/heptane mixture with increasing decalin composition, the C36c modification underestimates the same trend and is more accurate. The C36 maximum deviation at pure decalin is off by over 6% at maximum, whereas C36c is off by approximately 2% at maximum. Furthermore, while molar volumes are important, the decalin-self-energy and that with heptane are crucial to determine the enthalpic contribution to insertion/removal of cholesterol from various lipids. Since C36c agrees well with the molar excess enthalpy of decalin/heptane mixtures (Figure 2), this will likely extend to membranes with cholesterol with C36c. Interestingly, at low decalin compositions (<20%), C36 severely overestimates the excess molar enthalpy by as much as 1400% and then severely underestimates the excess molar enthalpy by as much as 480%. C36c slightly underestimates the molar excess enthalpy for most decalin compositions (<90%) and then slightly overestimates the molar excess enthalpy but, in general, is much closer to the experimental values than the C36. On the basis of this improved matching of experimental data, C36c was deemed to be an improvement over C36 for modeling decalin and heptane mixtures.

Although the decalin and heptane molecules comprise appropriate models for the ring structure of cholesterol and tails of lipids, C36c was found to have only a slight influence on some properties calculated for the three lipid bilayers. The C36 and C36c produced similar results in terms of SA per lipid, S_{CD} parameters, atomic form factors, and electron densities. The SAs per lipid only differed by 0.5 Å^2 or less, with the DMPC and 10% cholesterol simulations having statistically identical SAs per lipid. For all bilayers, the lipid chain S_{CD}s with 10% cholesterol with C36 and C36c were statistically identical. For the DMPC/30% cholesterol bilayer, the conditions for this mixture are near the liquid-ordered/liquid-disordered phase boundary at 298 K.[38] It appears that the force fields have slightly too much disorder as compared to experiment,[41] or the time scales for further chain ordering is more than the 100 ns time scale for the C36c simulations. However, there is a clear distinction between 10 and 30% cholesterol, i.e., an approximately constant S_{CD} in the middle of the chain for the elevated cholesterol bilayer.

The electron densities and atomic form factors also show similar results produced by C36 and C36c. The density profiles were virtually identical between the C36 and C36c except for DMPC/30% cholesterol, which showed differences in the methyl trough and phospholipid head regions. Both C36 and C36c matched experiment[39] extremely well in terms of form factors. Because of the similarities in results for the two force fields, and because both seem to match experiment almost equally well, previous cholesterol-containing bilayer simulations with C36 may be generally valid, at least in terms of SAs per lipid, deuterium order parameters, electron densities, and atomic form factors.

However, the cholesterol angle distributions were different between some of the C36 and C36c simulations. For the MD simulations of DMPC/10% cholesterol, the angle distribution was skewed more toward the upright orientation with C36c compared to C36. The mean was 20.6° and 22.5° for C36c and C36 and the difference in the mode was more pronounced with 15° and 21°, respectively. This is likely due to the favorable heat of mixing seen in C36c for low concentrations of decalin, which would lead to increased stacking of cholesterol against the acyl chains of the phospholipids. Furthermore, the trend observed in the C36c simulations is more pronounced than the trend observed using C36. While the mean angles are higher for C36 for all bilayers, the gap between DOPC/10% cholesterol and DMPC/10% cholesterol is greater for C36c than for C36, better illustrating the effect of unsaturation on cholesterol. In polyunsaturated fatty acids, a significant population of cholesterol has been shown to adopt an entirely parallel orientation relative to the bilayer surface.[42,43] While this is not observed in our simulations

of DOPC/10% cholesterol, there is still an increased tendency toward such an orientation due to DOPC's inability to form extended chains with which cholesterol preferentially interacts.

In many aspects, the C36c simulations result in similar bilayer properties as those with the original cholesterol force field.[17] Previous MD simulations of bilayers with cholesterol are likely to be reasonable with regards to accurate area per lipid, order parameters, and density profiles. However, the significant advance in this modified parameter set is cholesterol's self-interaction and that with the lipid acyl chains. On the basis of our decalin/heptane-based parametrization, the enthalpy and likely free energy of cholesterol in the hydrophobic core has changed. Therefore, simulations that study free energy for lipid flip/flop between leaflets will be different between C36 and C36c. This might explain the inability of previous work by Jo et al.[15] to calculate the preference of cholesterol for the center of a bilayer with polyunsaturated lipid chains.

In conclusion, a modification of the C36 force field (C36c) provides more accurate predictions of properties of decalin/heptane mixtures and, consequently, properties of bilayers containing cholesterol. The C36c modification results in better prediction of the molar volume and molar excess enthalpy of decalin/heptane mixtures, as shown by matching with experimental data. The C36c modification also results in better prediction of deuterium order parameters and atomic form factors of DMPC/cholesterol and supports expected trends regarding cholesterol position and orientation. This modification should ultimately prove useful in molecular modeling studies involving cholesterol, especially those focusing on cholesterol's attraction to lipids and proteins, such as cholesterol flip/flop between leaflets.

■ ASSOCIATED CONTENT

Supporting Information. Figures of the individual component density profiles for all bilayers, cholesterol, and decalin topology in CHARMM format, and tables with updated CHARMM force field parameters. This material is available free of charge via the Internet at http://pubs.acs.org.

■ AUTHOR INFORMATION

Corresponding Author

*Phone: (301) 405-1320. Fax: (301) 314-9126. E-mail: jbklauda@umd.edu.

■ ACKNOWLEDGMENT

This work was supported by institutional funding from the University of Maryland (J.B.K) and a Howard Hughes Medical Institute Undergraduate Research Fellowship (J.B.L). We would like to acknowledge Dr. George Khelashvili for providing us with the experimental form factors of the DMPC/30% cholesterol bilayer.

■ REFERENCES

(1) van Meer, G.; Voelker, D. R.; Feigenson, G. W. *Nat. Rev. Mol. Cell Biol.* **2008**, *9*, 112.
(2) Maxfield, F. R.; Tabas, I. *Nature* **2005**, *438*, 612.
(3) Wylie, J. L.; Hatch, G. M.; McClarty, G. *J. Bacteriol.* **1997**, *179*, 7233.
(4) Zelenka, P. S. *Curr. Eye Res.* **1984**, *3*, 1337.
(5) Jacob, R. F.; Cenedella, R. J.; Mason, R. P. *J. Biol. Chem.* **1999**, *274*, 31613.
(6) Pan, J.; Mills, T. T.; Tristram-Nagle, S.; Nagle, J. F. *Phys. Rev. Lett.* **2008**, *100*, 198103.
(7) Lingwood, D.; Simons, K. *Science* **2010**, *327*, 46.
(8) Pitman, M. C.; Grossfield, A.; Suits, F.; Feller, S. E. *J. Am. Chem. Soc.* **2005**, *127*, 4576.
(9) Khelashvili, G.; Pabst, G.; Harries, D. *J. Phys. Chem. B* **2010**, *114*, 7524.
(10) Pandit, S. A.; Jakobsson, E.; Scott, H. L. *Biophys. J.* **2004**, *87*, 3312.
(11) Pandit, S. A.; Vasudevan, S.; Chiu, S. W.; Mashl, R. J.; Jakobsson, E.; Scott, H. L. *Biophys. J.* **2004**, *87*, 1092.
(12) O'Connor, J. W.; Klauda, J. B. *J. Phys. Chem. B* **2011**, *115*, 6455.
(13) Risselada, H. J.; Marrink, S. J. *Proc. Natl. Acad. Sci. U.S.A.* **2008**, *105*, 17367.
(14) Bennett, W. F. D.; MacCallum, J. L.; Hinner, M. J.; Marrink, S. J.; Tieleman, D. P. *J. Am. Chem. Soc.* **2009**, *131*, 12714.
(15) Jo, S.; Rui, H.; Lim, J. B.; Klauda, J. B.; Im, W. *J. Phys. Chem. B* **2010**, *114*, 13342.
(16) Klauda, J. B.; Venable, R. M.; Freites, J. A.; O'Connor, J. W.; Mondragon-Ramirez, C.; Vorobyov, I.; Tobias, D. J.; MacKerell, A. D.; Pastor, R. W. *J. Phys. Chem. B* **2010**, *114*, 7830.
(17) Pitman, M. C.; Suits, F.; MacKerell, A. D.; Feller, S. E. *Biochemistry* **2004**, *43*, 15318.
(18) Vanommeslaeghe, K.; Hatcher, E.; Acharya, C.; Kundu, S.; Zhong, S.; Shim, J.; Darian, E.; Guvench, O.; Lopes, P.; Vorobyov, I.; et al. *J. Comput. Chem.* **2010**, *31*, 671.
(19) Frisch, M. J.; Trucks, G. W.; Schlegel, H. B.; Scuseria, G. E.; Robb, M. A.; Cheeseman, J. R.; Montgomery, J. A., Jr.; Vreven, T.; Kudin, K. N.; Burant, J. C.; Millam, J. M.; Iyengar, S. S.; Tomasi, J.; Barone, V.; Mennucci, B.; Cossi, M.; Scalmani, G.; Rega, N.; Petersson, G. A.; Nakatsuji, H.; Hada, M.; Ehara, M.; Toyota, K.; Fukuda, R.; Hasegawa, J.; Ishida, M.; Nakajima, T.; Honda, Y.; Kitao, O.; Nakai, H.; Klene, M.; Li, X.; Knox, J. E.; Hratchian, H. P.; Cross, J. B.; Bakken, V.; Adamo, C.; Jaramillo, J.; Gomperts, R.; Stratmann, R. E.; Yazyev, O.; Austin, A. J.; Cammi, R.; Pomelli, C.; Ochterski, J. W.; Ayala, P. Y.; Morokuma, K.; Voth, G. A.; Salvador, P.; Dannenberg, J. J.; Zakrzewski, V. G.; Dapprich, S.; Daniels, A. D.; Strain, M. C.; Farkas, O.; Malick, D. K.; Rabuck, A. D.; Raghavachari, K.; Foresman, J. B.; Ortiz, J. V.; Cui, Q.; Baboul, A. G.; Clifford, S.; Cioslowski, J.; Stefanov, B. B.; Liu, G.; Liashenko, A.; Piskorz, P.; Komaromi, I.; Martin, R. L.; Fox, D. J.; Keith, T.; Al-Laham, M. A.; Peng, C. Y.; Nanayakkara, A.; Challacombe, M.; Gill, P. M. W.; Johnson, B.; Chen, W.; Wong, M. W.; Gonzalez, C.; Pople, J. A. *Gaussian 03*, revision B.03; Gaussian, Inc.: Wallingford, CT, 2003.
(20) Brooks, B. R.; Brooks, C. L.; Mackerell, A. D.; Nilsson, L.; Petrella, R. J.; Roux, B.; Won, Y.; Archontis, G.; Bartels, C.; Boresch, S.; et al. *J. Comput. Chem.* **2009**, *30*, 1545.
(21) Jo, S.; Kim, T.; Iyer, V. G.; Im, W. *J. Comput. Chem.* **2008**, *29*, 1859.
(22) Jo, S.; Lim, J. B.; Klauda, J. B.; Im, W. *Biophys. J.* **2009**, *97*, 50.
(23) Phillips, J. C.; Braun, R.; Wang, W.; Gumbart, J.; Tajkhorshid, E.; Villa, E.; Chipot, C.; Skeel, R. D.; Kale, L.; Schulten, K. *J. Comput. Chem.* **2005**, *26*, 1781.
(24) Darden, T.; York, D.; Pedersen, L. *J. Chem. Phys.* **1993**, *98*, 10089.
(25) Hoover, W. G. *Phys. Rev. A* **1985**, *31*, 1695.
(26) Nosé, S.; Klein, M. L. *J. Chem. Phys.* **1983**, *78*, 6928.
(27) Andersen, H. C. *J. Chem. Phys.* **1980**, *72*, 2384.
(28) Klauda, J. B.; Wu, X. W.; Pastor, R. W.; Brooks, B. R. *J. Phys. Chem. B* **2007**, *111*, 4393.
(29) Klauda, J. B.; Venable, R. M.; MacKerell, A. D.; Pastor, R. W. Considerations for Lipid Force Field Development. In *Computational Modeling of Membrane Bilayers*; Academic Press: New York, 2008; Vol. 60, p 1.
(30) Klauda, J. B.; Brooks, B. R.; MacKerell, A. D., Jr.; Venable, R. M.; Pastor, R. W. *J. Phys. Chem. B* **2005**, *109*, 5300.

(31) Wu, X. W.; Brooks, B. R. *J. Chem. Phys.* **2005**, *122*, 044107.
(32) Feller, S. E.; Zhang, Y.; Pastor, R. W.; Brooks, B. R. *J. Chem. Phys.* **1995**, *103*, 4613.
(33) Martyna, G. J.; Tobias, D. J.; Klein, M. L. *J. Chem. Phys.* **1994**, *101*, 4177.
(34) Lide, D. R. *CRC Handbook*, 81st ed.; CRC Press: Boca Raton, FL, 2000.
(35) Fujihara, I.; Kobayashi, M.; Murakami, S. *J. Chem. Thermodyn.* **1983**, *15*, 1.
(36) Fujihara, I.; Kobayashi, M. *Fluid Phase Equilib.* **1983**, *15*, 81.
(37) Klauda, J. B.; Garrison, S. L.; Jiang, J.; Arora, G.; Sandler, S. I. *J. Phys. Chem. A* **2004**, *108*, 107.
(38) Almeida, P. F. F.; Vaz, W. L. C.; Thompson, T. E. *Biochemistry* **1992**, *31*, 6739.
(39) Hodzic, A.; Rappolt, M.; Amenitsch, H.; Laggner, P.; Pabst, G. *Biophys. J.* **2008**, *94*, 3935.
(40) Dufourc, E. J.; Parish, E. J.; Chitrakorn, S.; Smith, I. C. P. *Biochemistry* **1984**, *23*, 6062.
(41) Douliez, J. P.; Leonard, A.; Dufourc, E. J. *Biophys. J.* **1995**, *68*, 1727.
(42) Harroun, T. A.; Katsaras, J.; Wassall, S. R. *Biochemistry* **2006**, *45*, 1227.
(43) Harroun, T. A.; Katsaras, J.; Wassall, S. R. *Biochemistry* **2008**, *47*, 7090.